Proceedings of the 11th ICPMG 2026
11th International Conference on Physical Modelling in Geotechnics
8-12 June 2026, Zurich, Switzerland

Centrifuge modelling of seismically loaded monopiles: DONISIS – Model Creation and Site Response

L.A. Jones, E. Brunschweiler
ETH Zürich, Zürich, Switzerland, jonesli@ethz.ch, beva@ethz.ch

S. Panagoulias,
TU Delft, Delft, the Netherlands, s.panagoulias@tudelft.nl
Siemens Energy, Rijswijk, the Netherlands, stavros.panagoulias@siemens-energy.com

F. Pisanò
NGI, Boston, Massachusetts, federico.pisano@ngi.no

E. Kementzetzidis
TU Delft, Delft, the Netherlands, e.kementzetzidis@tudelft.nl

I. Anastasopoulos
ETH Zürich, Zürich, Switzerland, ixa@ethz.ch

ABSTRACT: Increasing demand for offshore wind energy is driving the need for ever larger offshore wind turbines (OWTs) in more challenging environments, including seismically active regions. The effects of earthquake loading on large diameter monopiles supporting OWTs is therefore an increasingly relevant topic, requiring further investigation. Such structures can be physically modelled in a geotechnical centrifuge. Such modelling requires correct simulation of both dynamic soil and structural response, as well as the reproduction of excess pore water pressure (EPWP) generation. Several advanced modelling techniques are required to produce reliable results. This work presents the detailed preparation, construction and design of such an experimental campaign for a large diameter monopile supporting an OWT in liquefiable soil. The soil is prepared using a viscous fluid solution for proper scaling of permeability, and is instrumented with pore pressure transducers (PPTs) and displacement sensors. The soil layer is constructed within a special laminar box, which reproduces boundary conditions consistent with 1-D seismic wave propagation. Results show that the mobilised soil properties can be deduced from the recorded site response, strain level leads to a change in system response and significant pore pressures can develop even when soil permeability is overestimated.

1 INTRODUCTION

The determination of seismic site response is a key component of geotechnical modelling. A model soil column is created within a *laminar box*, whose behaviour mimics free-field conditions for vertically propagating seismic waves, minimising or eliminating interference from the lateral boundaries. Two configurations are investigated; "high permeability"; saturated with water, approximating "drained" conditions, and "low-permeability"; saturated with a correctly scaled viscous fluid, producing the correct prototype permeability and thus excess pore water generation. An array of accelerometers and pore pressure transducers are placed within the soil and the system is excited using a 1D shake table. The response is recorded, and the site properties such as site period, shear-wave velocity profile, excess pore pressures and shear strain profile are deduced. While in principle a

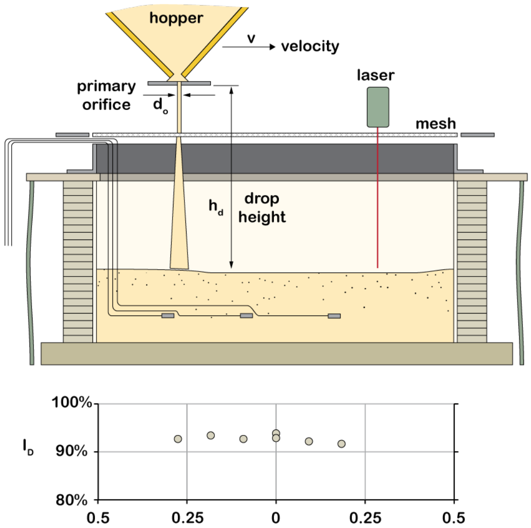

Figure 1. Schematic overview of model box and sand raining as well as measured achieved density (I_D) within the box.

straightforward test, steps must be taken to ensure that the soil column is well defined, properly saturated and instrumented. Presented here is a model of a soil deposit composed of uniform dense Hostun (HN31) sand, fully saturated and having a depth of h This model forms the basis for further tests employing a large diameter monopile and an OWT superstructure as part of project DONISIS (Pisanò et al., 2024).

2 MODEL PREPARATION

The model is prepared using a curtain-type air pluviation technique, employing the ETH automatic pluviation system (Fig. 1). Initially stored in a large 1.5t capacity hopper, the sand passes through an initial large opening, and then between two precisely aligned aluminium plates, which function as the primary orifice for controlling mass-flow.

The primary orifice has a slit-opening d_0 with accuracy of +-0.1mm, measured using feeler-gauges. The automated sand raining system maintains a precise travel velocity (v) and drop height (h_d) above the sand surface (Fig. 1). An additional coarse diffuser mesh (passing diameter d_m) is placed above the laminar box, helping to minimize shadowing effects close to the lateral boundaries of the box. The diffuser mesh remains at a fixed height; the drop height measured between the primary orifice and sand surface was found to be the most critical parameter, for this density. The system is first calibrated to derive the optimum settings (drop height, speed, opening, diffuser-mesh) for the target relative density I_D = 95% (Table 1).

Table 1 Final pluviator settings for the target density 95%.

$\boldsymbol{h_d}$	$\boldsymbol{v}$	$\boldsymbol{d_o}$	$\boldsymbol{d_m}$
700mm	10 mm/s	1.2 mm	1.9 mm

This calibration is performed by placing an array of small "calibration" pots throughout the box, whose mass and volume are precisely known. A layer of sand is pluviated, the pots recovered and the mass of material in each pot is determined. In this way, both the general trends (e.g. drop height vs. void ratio) as well as the variability of the achieved density within the box can be deduced (Fig. 1). For the chosen model, this corresponds to an average relative density of 90% with a variability of 5% throughout the depth and width of the box; the short edges of the box being slightly looser than the middle. Repeatability is within 2% I_D for the same pot placed in the same location, which is comfortably within the physical error in the measurement.

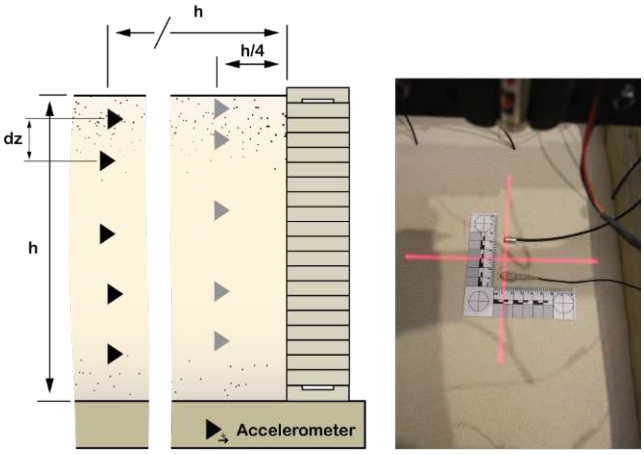

Figure 2. Layout of accelerometers within the model: two vertical arrays are shown, at the centre and towards the boundary of the box.

2.1 Laminar Box

The model is constructed within a specialised, in house built "Laminar" box, which replicates free-field boundary conditions for vertically propagating shear waves in a soil stratum (Hushmand et al., 1988). The box is made up of 20 "shear rings" stacked on-top of each other, with linear roller bearings between each layer. In such a way, the soil is allowed to deform in the direction of shaking, while still being confined against bulging. The shear rings are constructed of hardened aluminium, and the shear ring-linear bearing assembly has a measured inter-layer friction coefficient of less than 1%. Each ring weighs 6kg, which affects the dynamic response of the soil column: an effect that can be modelled reliably by assuming an increased soil mass, approximately 35% for a fully saturated sand. This value is calculated based on the ratio of the mass of each ring plus the mass of soil contained within against the mass of soil $(m_{soil} + m_{ring})/m_{soil}$, assuming a saturated sand of unit weight $20kN/m^3$. An internal latex membrane provides water-tightness while minimally affecting the soil response. Saturation is achieved through bronze filter plates in the bottom of the box, which are supplied via internal water passages in the base plate of the box.

3 INSTRUMENTATION

The model is instrumented with piezoelectric accelerometers and pore pressure transducers (PPTs) in addition to the accelerometers lasers and LVDTs mounted on the box and shaking table. Sensors are installed in layers during pluviation. The actual achieved position of each sensor is measured and

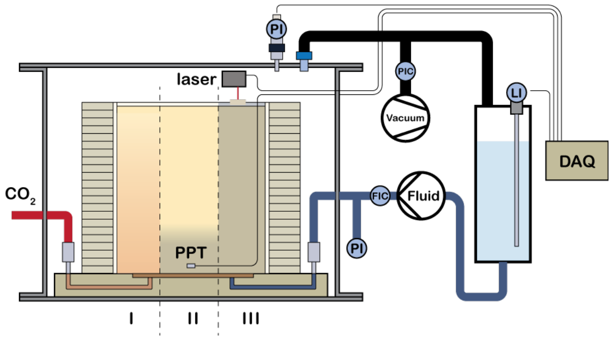

Figure 3. Schematic representation of saturation process including the three main streps: (I) CO2 cycling; (II) saturation; and (III) saturation ratio determination.

recorded during model preparation using a laser measuring system (Fig. 2).

4 SATURATION

The model is saturated through a multistep procedure, following the process outlined by Okamura & Inoue (2012). The filled laminar box is initially placed within a large vacuum chamber (Fig. 3). The bottom filter of the laminar box is connected to the outside of the box through a tube valve system.

The air in the chamber is first evacuated down to a pressure of -0.9 Bar. The chamber is then re-pressurized using dry CO_2 via the filter, ensuring any air and moisture is pushed out of the soil matrix. Throughout this process, the pressure is monitored by pressure indicators (PI): one in the chamber, one connected to the filter, and one of the PPTs already in the soil. Attention should be paid to avoid fluidising the soil using the CO_2.. Once the gas pressure is approximately equal to atmosphere, Vacuum is applied again, and the entire process is repeated at least 2 times.

Viscous fluid (methylcellulose solution) or de-aired water is prepared in a separate vacuum mixer following the procedures outline by Adamidis & Madabhushi (2015) and Stewart et al., (1998). The viscosity of the resulting fluid is measured using a bench-top viscometer (Lamy Rheology B-ONE PLUS with DIN-19 attachment), while the temperature is monitored and recorded through a thermal camera. The vacuum mixer and the vacuum chamber share the same, pressure regulated (PIC) supply of vacuum, which is large enough to accommodate significant leaks in either vessel, ensuring pressure is always equal in the two containers. The pressure is set to 0.5-0.8 bar (absolute) throughout the saturation process. The viscous fluid is supplied to the filter of the laminar box by a flow-controlling (FIC) peristaltic pump (Lead Fluid WG600F), which supplies a precise volume of fluid per second. The safe flux to avoid fluidisation is calculated using the simple Darcy equation and an estimate of the soil's hydraulic conductivity and the measured fluid viscosity (Stringer & Madabhushi, 2009). A safety factor of 2 is applied to the calculated safe flux to avoid fluidisation and the actual pressures in both the filter and the pores are continuously logged by the data acquisition system (DAQ). The level of fluid within the tank is similarly logged with a level indicator (LI) to confirm the function of the flow regulating pump. The actual performance of the pump is dependent on the pressure inside the fluid line and should be calibrated at the reference vacuum pressure.

Once the CO_2 cycles are complete, the chamber pressure is set and the pump started, the saturation continues autonomously, only requiring occasional supervision to take manual measurements of tank volume. Depending on the viscosity, saturation may take several days. The pressures in the box, the fluid pressures and the tank level are continuously logged by the DAQ during this time, and can be used later to compare expected vs. achieved permeability and volume of pores, which can give an additional indication of the achieved void ratio. The model is saturated until the free water level is approximately 10 mm above the sand surface.

Once saturation is complete, the saturation ratio can be estimated through the process proposed by Okamura & Inoue (2012). A high precision laser (MikroEpsilon ILD-200-25) is focused on a floating target placed on the free surface of water in the model box. The vacuum pressure in the chamber is then adjusted by 0.2 bar (from -0.5 to -0.3 bar) and the change in height of the water surface (if any) is recorded. This change in apparent fluid volume can be correlated with the air in the pores of the sand and thus the saturation ratio.

5 SITE RESPONSE

Once saturation has been completed, the model is weighed and placed on the centrifuge for testing. The laminar box is bolted to the shaking table through high-strength prestressed bolts and vibration resisting safety washers to ensure adequate coupling between table and payload. The model is spun-up to achieve the target g-level at the reference height ($h/2$) within the box, and the seismic motion is applied.

The behaviour of the soil column is highlighted through examination of the array of accelerometers in the soil (Fig. 4). Small windows of the acceleration time histories are first extracted from each sensor,. Points of inflection and local peaks are identified in each window. These time points are compared between sensors, allowing the determination of a seismic travel-time (dt) between sensors. The vertical distance between the sensors (dz) is then computed based on the measured position from installation. Assuming vertically propagating shear waves, the local average shear wave velocity (v_s) is then determined as $v_s = dz/dt$. Two pulses, a low amplitude (light) and high amplitude (dark) are highlighted in Fig. 4. The computed average shear wave velocity between pairs of sensors is plotted at mid-depth between each sensor, producing a mobilised or effective shear wave velocity profile, which is a function of amplitude and depth. The known initial void ratio and depth can also be used to compute an initial, or elastic (small strain) shear wave velocity profile (Azeiteiro et al., 2017). Double integration of the acceleration time history for each sensor produces a displacement (d) profile for the same time points. This can in turn be converted to a shear-strain (γ) profile and compared with a G-modulus reduction curve from literature (Ishibashi & Zhang, 1993) to produce an effective stiffness ratio profile. Comparison of the measured shear wave velocity, the expected elastic velocity and the estimated G-reduction reveals similar trends, with large strains close to the surface producing drastically reduced local shear wave velocity.

Along with the accelerometers, PPTs are placed in a similar array. Two tests are compared: one with correctly scaled "viscous fluid" (methylcellulose solution) and one simply with water. Both are fully saturated using the same procedure (as outlined earlier), and subjected to the same input motion. The two models are identical with the exception of the viscosity of the pore fluid. As expected, increasing the viscosity is equivalent to reducing the permeability of the soil. Pore pressure generation in one of the upper layers is shown in Fig. 5a. Initially, the cycle-to cycle accumulation of pore pressure is similar. However, in the "high permeability" case, this pressure dissipates quickly, while in the "low permeability" case the excess pore water pressures continue to accumulate. This has an effect on the motion transmitted through the soil column, and the near-surface ($z \approx 2m$) response spectrum of acceleration, $Se(T/T_1)$, is clearly affected by the generation of excess pore water pressures (Fig. 5b).

The water saturated model has a larger PGA and shows stronger response across the entire frequency range. To illustrate this, the ratio of the input (outcrop) response spectrum Se_b to the response spectrum at depth z=16m, $Se(z)$ produces the Soil Factor (EC8-2004)

$$S = Se(z)/Se_b \qquad (1)$$

Comparing the two models (Fig. 5c), the water saturated model exhibits *amplification* of the input motion everywhere in the spectrum, while the viscous fluid model has *de-amplification* of the peak ground acceleration, as well as less amplification through the entire frequency range. This is despite the model being very dense and full liquefaction ($r_u = 1$) never occurring. In addition to the additional damping provided by significant pore pressure generation; the excess pore pressures may lower the effective stress,

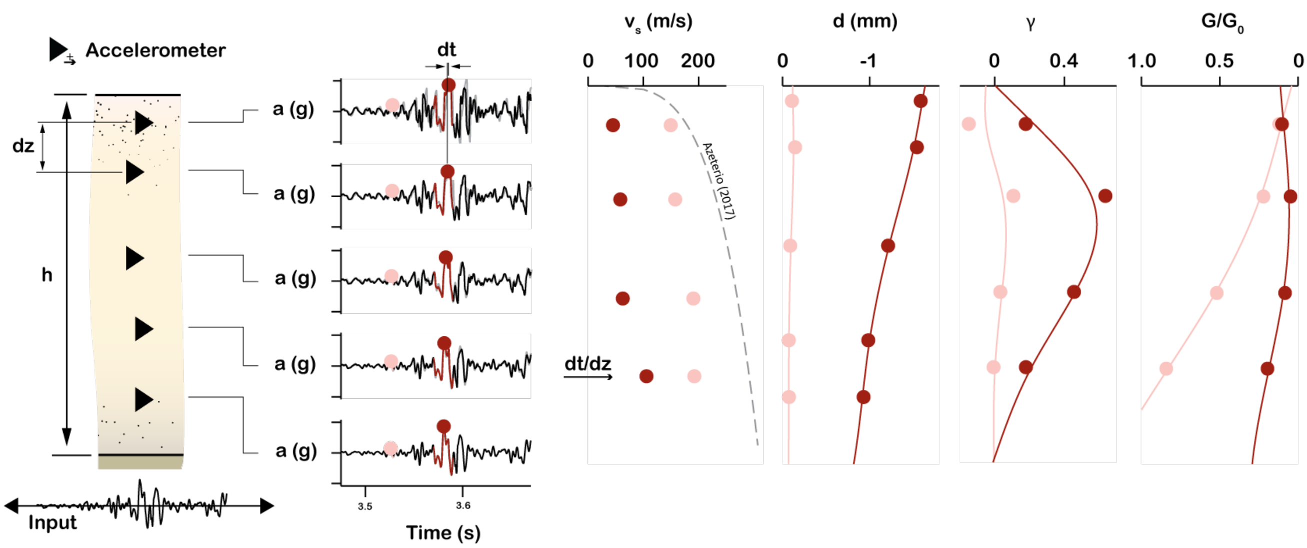

Figure 4. Deduction of site properties from the central array of accelerometers within the model. From left to right: sensor positions, acceleration time histories (lowpass filter 500Hz), points of computed shear wave velocity, displacement, shear strain and stiffness reduction with fitted curves for visualisation.

reducing soil stiffness and "detuning" the soil column, strengthening the nonlinear response of the soil.

6 CONCLUSIONS

Soil models for seismic centrifuge tests are created using an automated sand raining system, which produces repeatable and controllable, uniform sand profiles in a specialised laminar box. The model is instrumented and saturated following a multistep procedure including CO_2 cycling and saturation ratio determination. The models created produce high quality data which can be used to determine system level response of a soil column subjected to seimic shaking. The effects of shear strain softening and pore pressure generation can be seen to be important even for very dense sands subjected to relatively moderate seismic shaking.

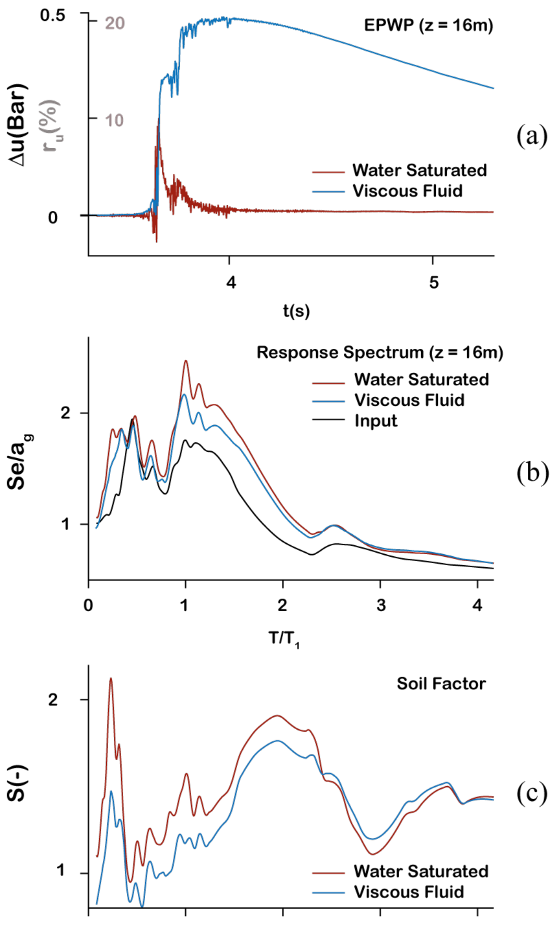

Figure 5 (a) Excess pore water at the same location in the two models, (b) response spectrum Se and (c) soil factor S for the same models against normalised period T/T_1 where T_1 is the first elastic period of the soil column.

ACKNOWLEDGEMENTS

The authors thank M. Iten, J. Giger, S. Barbieri, A. Kieper and R. Herzog for their technical support.

The DONISIS project is funded by the Dutch Research Council (NWO) under the Open Technology Programme (OTP) – number: 19882; grant recipients: TU Delft, ETH Zürich. Co-funding and/or technical support is provided by Carbon Trust, further information about insdustry partners and collaborators can be found using the QR code:

REFERENCES

Adamidis, O., & Madabhushi, G. S. P. (2015). Use of viscous pore fluids in dynamic centrifuge modelling. *International Journal of Physical Modelling in Geotechnics*, *15*(3), 141–149. https://doi.org/10.1680/IJPMG.14.00022

Azeiteiro, R. J. N., Coelho, P. A. L. F., David, ;, Taborda, M. G., & Grazina, J. C. D. (2017). Critical State–Based Interpretation of the Monotonic Behavior of Hostun Sand. *Journal of Geotechnical and Geoenvironmental Engineering*, *143*(5), 04017004. https://doi.org/10.1061/(ASCE)GT.1943-5606.0001659

CEN. (2004). *Eurocode 8: Design of structures for earthquake resistance – Part 1: General rules, seismic actions and rules for buildings* (Issue EN 1998-1:2004). CEN.

Hushmand, B., Scott, R. F., & Scott, R. F. (1988). Centrifuge liquefaction tests in a laminar box. *Géotechnique*, *38*(2), 253–262. https://doi.org/10.1680/GEOT.1988.38.2.253

Ishibashi, I., & Zhang, X. (1993). UNIFIED DYNAMIC SHEAR MODULI AND DAMPING RATIOS OF SAND AND CLAY. *SOILS AND FOUNDATIONS*, *33*(1), 182–191. https://doi.org/10.3208/SANDF1972.33.182

Okamura, M., & Inoue, T. (2012). Preparation of fully saturated models for liquefaction study. *International Journal of Physical Modelling in Geotechnics*, *12*(1), 39–46. https://doi.org/10.1680/IJPMG.2012.12.1.39

Pisanò, F., Panagoulias, S., Anastasopoulos, I., Kaynia, A., Petalas, A., Brasile, S., Page, A., Kementzetzidis, E., & Metrikine, A. V. (2024). DONISIS: Design of Offshore moNopiles Including Seismic Interaction with Soil. *Japanese Geotechnical Society Special Publication*, *10*(36), 1383–1388. https://doi.org/10.3208/JGSSP.V10.OS-25-05

Stewart, D. P., Chen, Y.-R., & Kutter, B. L. (1998). Experience with the Use of Methylcellulose as a Viscous Pore Fluid in Centrifuge Models. *Geotechnical Testing Journal* , *21*(4), 365–369. https://doi.org/10.1520/GTJ11376J

Stringer, M. E., & Madabhushi, S. P. G. (2009). Novel Computer-Controlled Saturation of Dynamic Centrifuge Models Using High Viscosity Fluids. *Geotechnical Testing Journal* , *32*(6), 559–564. https://doi.org/10.1520/GTJ102435